LETTER

doi:10.1038/nature11833

Non-optimal codon usage affects expression, structure and function of clock protein FRQ

Mian Zhou[1], Jinhu Guo[1]†, Joonseok Cha[1], Michael Chae[1], She Chen[2], Jose M. Barral[3], Matthew S. Sachs[4] & Yi Liu[1]

Codon-usage bias has been observed in almost all genomes and is thought to result from selection for efficient and accurate translation of highly expressed genes[1–3]. Codon usage is also implicated in the control of transcription, splicing and RNA structure[4–6]. Many genes exhibit little codon-usage bias, which is thought to reflect a lack of selection for messenger RNA translation. Alternatively, however, non-optimal codon usage may be of biological importance. The rhythmic expression and the proper function of the *Neurospora* FREQUENCY (FRQ) protein are essential for circadian clock function. Here we show that, unlike most genes in *Neurospora*, *frq* exhibits non-optimal codon usage across its entire open reading frame. Optimization of *frq* codon usage abolishes both overt and molecular circadian rhythms. Codon optimization not only increases FRQ levels but, unexpectedly, also results in conformational changes in FRQ protein, altered FRQ phosphorylation profile and stability, and impaired functions in the circadian feedback loops. These results indicate that non-optimal codon usage of *frq* is essential for its circadian clock function. Our study provides an example of how non-optimal codon usage functions to regulate protein expression and to achieve optimal protein structure and function.

Eukaryotic circadian oscillators consist of autoregulatory circadian negative-feedback loops. In the core circadian oscillator of *Neurospora crassa*, FRQ protein is a central component that functions as the circadian negative element with its partner FRH[7–9]. Two transcription factors, WHITE COLLAR (WC)-1 and WC-2, form a heterodimeric complex that activates *frq* transcription[10]. The FRQ–FRH complex inhibits WC complex activity by interacting with the WC proteins[11,12]. The level and stability of FRQ have a key role in setting period length, phase and clock sensitivity to environmental signals[7,8,13]. In addition, FRQ promotes the expression of both WC proteins in an interlocked positive-feedback loop[10,14].

The protein-coding genes of *Neurospora* exhibit strong codon bias (Supplementary Fig. 1a). The third position of almost every codon family in this filamentous fungus has the preference C>G>T>A. Codon optimization enhances the expression of a heterologous luciferase gene in *Neurospora*[15,16]. To establish that codon-usage bias regulates protein expression, we identified the most abundant *Neurospora* proteins in a whole-cell extract by mass spectrometry analyses. The genes encoding the top 100 most abundant proteins (Supplementary Table 1) exhibit much stronger codon bias than the rest of the protein-coding genes (Supplementary Fig. 1b).

We classified all predicted *Neurospora* transfer RNA genes and predicted the relative translation elongation rate for each codon on the basis of tRNA-gene copy numbers, which correlate with tRNA abundance, and the nature of anticodon–codon interactions[4,17]. The most preferred codon for each amino acid is always the codon with highest predicted translation elongation rate (Supplementary Table 2). Therefore, to ensure efficient translation of abundant proteins, selection pressure favoured a bias for codons translated by highly abundant tRNA species.

Many *Neurospora* genes exhibit little or no codon bias (Supplementary Fig. 1a). FRQ is a low-abundance *Neurospora* protein. Its codon bias index[18] (CBI; in which CBI = 0 indicates completely random codon usage) value of 0.08 indicates that *frq* has little codon bias (Supplementary Fig. 1b). A codon-usage graph of the *frq* open reading frame (ORF) shows that many regions have non-optimal usage (Fig. 1a), whereas *frh* has good codon usage throughout its ORF.

We created two constructs in which the amino-terminal end (amino acids 1–164) of *frq* was codon optimized. In the m-*frq* construct, only the non-preferred codons were changed, whereas every codon was optimized in the f-*frq* construct. Predicted stability of RNA secondary structure was not notably affected by the optimization (Supplementary Table 3). These constructs and the wild-type *frq* (wt-*frq*) gene were transformed individually into a *frq* null strain (frq^{10}). Both m-*frq* and f-*frq* strains have significantly higher levels of FRQ proteins in constant light than that of the wt-*frq* strain (Fig. 1b and Supplementary Fig. 2a). On the other hand, *frq* mRNA levels were comparable in these strains (Supplementary Fig. 2b). FRQ is known to upregulate WC protein levels[10,14]. The WC-1 and WC-2 levels, however, were similar in these strains despite the much higher levels of FRQ in the optimized strains (Fig. 1b and Supplementary Fig. 2a, c).

The wt-*frq* construct was able to fully rescue the arrhythmic conidiation rhythm of the frq^{10} strain in constant darkness (Fig. 1c), but both of the optimized *frq* strains exhibited arrhythmic conidiation phenotypes; these are not due to the modest changes in the ratios of two alternatively translated FRQ forms, as either form of FRQ alone can support robust rhythms[19,20].

We created two additional constructs (m1-*frq* and m2-*frq*), in which only the amino- or carboxy-terminal segments of the optimized region of m-*frq*, respectively, were optimized. The frq^{10} transformants carrying either construct exhibited long-period conidiation rhythms and had FRQ levels between those of wt-*frq* and m-*frq* strains (Fig. 1c and Supplementary Fig. 3a). These results indicate that the severe conidiation rhythm phenotypes of the m-*frq* and f-*frq* strains are due to the cumulative effect of codon optimization and are not likely due to mutation of a DNA or RNA element.

To examine circadian phenotypes at the molecular level, we introduced a luciferase reporter construct that is under the control of the *frq* promoter[16] into wt-*frq*, m-*frq* and f-*frq* strains. As shown in Fig. 1d and Supplementary Fig. 3b, the robust rhythmic luciferase activity was abolished in the optimized strains. FRQ protein levels also lost molecular rhythmicity in the optimized strains (Fig. 1e, f and Supplementary Fig. 3c, d): the overall levels of FRQ were high and circadian changes in FRQ abundance and phosphorylation profile were abolished. In addition, FRQ stayed hyperphosphorylated in constant darkness in the optimized strains. Together, these results indicate that the non-optimal codon usage of *frq* governs FRQ expression level and is essential for clock function.

[1]Department of Physiology, The University of Texas Southwestern Medical Center, 5323 Harry Hines Boulevard, Dallas, Texas 75390, USA. [2]National Institute of Biological Sciences, 7 Life Science Park Road, Changping District, Beijing 102206, China. [3]Departments of Neuroscience and Cell Biology and Biochemistry and Molecular Biology, The University of Texas Medical Branch, Galveston, Texas 77555-0620, USA. [4]Department of Biology, Texas A&M University, College Station, Texas 77843-3258, USA. †Present address: State Key Laboratory of Biocontrol, School of Life Sciences, Sun Yat-sen University, Guangzhou 510275, China.

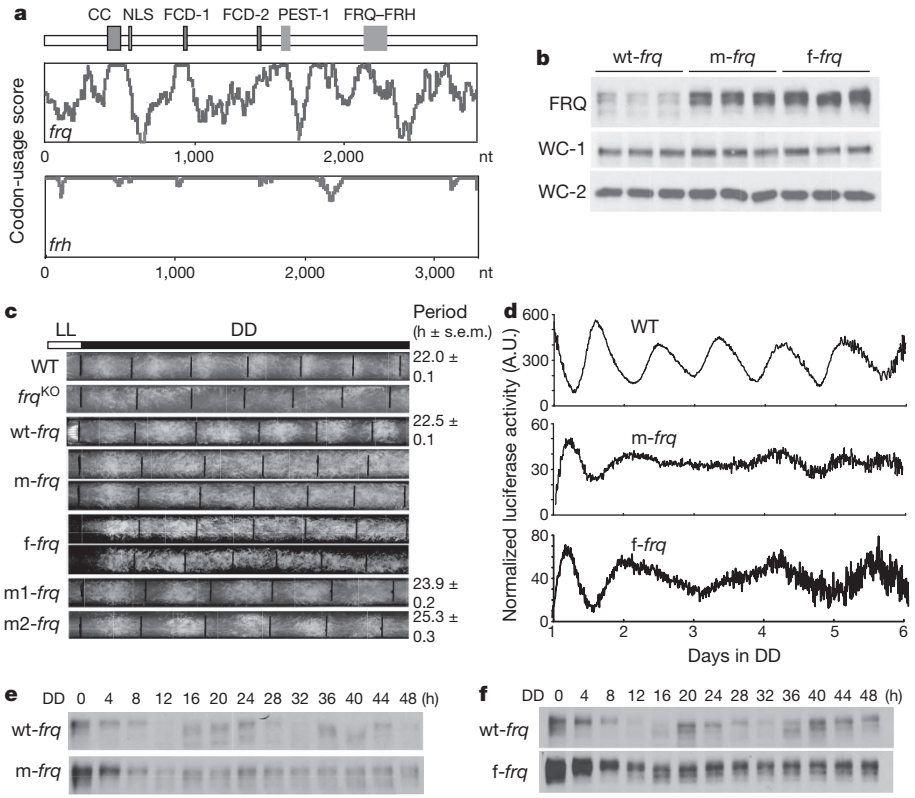

Figure 1 | Codon optimization of *frq* results in high FRQ expression levels and loss of circadian rhythmicities. **a**, Codon-usage score plots of *frq* and *frh* obtained using Codon Usage 3.5. CC, coiled-coil domain; FCD, FRQ–CK1 interaction domain; FRQ–FRH, FRQ–FRH interaction domain; NLS, nuclear-localization signal; nt, nucleotide; PEST, proline (P), glutamic acid (E), serine (S) and threonine (T) domain. **b**, Western blot showing the levels of FRQ and WC proteins in wt-*frq*, m-*frq* and f-*frq* strains. Three independent cultures in constant light at 25 °C were used. **c**, Race tube analysis showing the conidiation phenotypes in constant darkness (DD). Black lines indicate the growth fronts every 24 h. LL, constant light. **d**, Luciferase reporter assay showing *frq* promoter activity of the indicated strains after 1 day in constant darkness. The measurement of luciferase activity was normalized to subtract the baseline luciferase signal. A.U., arbitrary units. **e**, **f**, Western blots showing loss of FRQ expression rhythms in the codon-optimized strains in DD.

The loss of circadian rhythms in the optimized strains is surprising, as we previously showed that high FRQ levels do not result in arrhythmicity[10,21], suggesting that codon optimization causes defects in FRQ function. FRQ fulfils its function in the circadian negative-feedback loop through its interaction with WC proteins[11]. Immunoprecipitation assays showed that the relative amounts of FRQ associated with WC-2 were significantly decreased in both optimized strains (Fig. 2a), suggesting that the FRQ function in the negative-feedback loop is impaired in the optimized strains.

FRQ also acts in a positive-feedback loop by promoting WC protein expression[10,14]. Constructs qa-m-*frq* and qa-f-*frq*, in which either m-*frq* or f-*frq* is under the control of a quinic-acid-inducible promoter, respectively, were introduced into the *frq* null strain. As expected, FRQ levels were higher in the qa-m-*frq* and qa-f-*frq* strains than the control

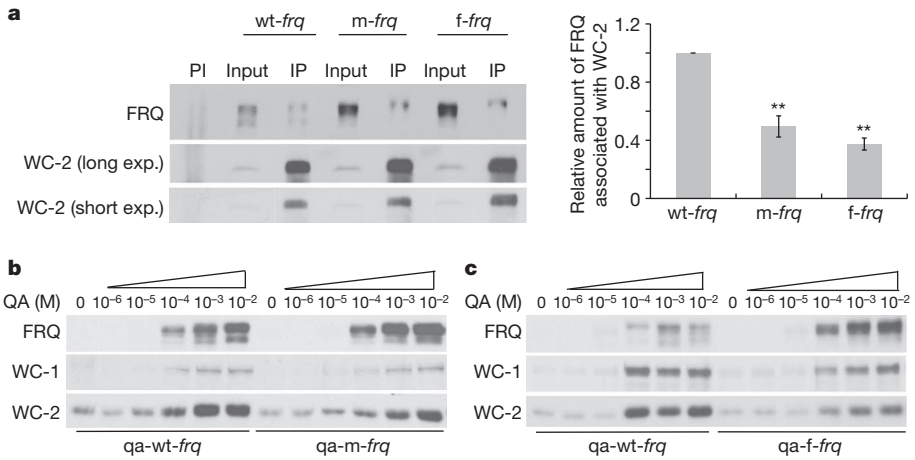

Figure 2 | FRQ activities in circadian feedback loops are impaired in the *frq* codon-optimized strains. **a**, Left, immunoprecipitation assay showing that FRQ has a decreased ability to interact with WC-2 in the codon-optimized strains. Two different exposures (exp.) of the WC-2 western blot were shown. Right, densitometric analyses of results from four independent experiments. IP, immunoprecipitation; PI, pre-immune serum. Error bars denote ± s.e.m. ($n = 9$). $^{**}P < 0.01$. **b**, **c**, Western blots showing the levels of WC proteins and FRQ in the indicated strains at different concentrations of quinic acid (QA) in constant light.

qa-wt-*frq* strain at a given quinic acid concentration (Fig. 2b, c and Supplementary Figs 4 and 5). Induction of FRQ resulted in increased levels of WC proteins, demonstrating the role of FRQ in the positive-feedback loop. At quinic acid concentrations higher than 1×10^{-4} M, however, the qa-m-*frq* and qa-f-*frq* strains had lower levels of WC-1 and WC-2 than the qa-wt-*frq* strain, despite having higher FRQ levels, indicating that FRQ function in the positive-feedback loop is also impaired in the codon-optimized strains.

The fact that FRQ function is impaired in codon-optimized strains despite higher FRQ protein levels suggests that the structural conformation of FRQ is altered. FRQ becomes progressively phosphorylated before its degradation[7]. Figure 3a shows that, in both m-*frq* and f-*frq* strains, FRQ was less stable than in the wild-type strain after the addition of cycloheximide (CHX). The difference in FRQ stability was most pronounced after 3 h of CHX treatment, a time when FRQ became hyperphosphorylated.

FRQ from the optimized strains was also less stable after protein extraction *in vitro* after freeze–thaw cycles. Although FRQ levels in freshly isolated samples were significantly higher in optimized strains, they decreased rapidly after freeze–thaw cycles (Fig. 3b). By contrast, expression of wt-*frq* in a *wc-2* knock-out strain to a level that is comparable to that of the optimized *frq* strains did not affect the freeze–thaw sensitivity of FRQ (Supplementary Fig. 6), indicating that the change in FRQ stability in the optimized strains is not due to high FRQ level or its reduced ability to interact with WC proteins. Furthermore, limited trypsin digestion showed that full-length FRQ in either optimized strain was more sensitive to trypsin digestion than in the control strain (Fig. 3c).

We reasoned that the changes in FRQ conformation in the optimized strains are due to an increase in the translation rate as a result of codon optimization. Thus, we examined whether FRQ in the f-*frq* strain can be rescued by the decreasing protein-translation rate at

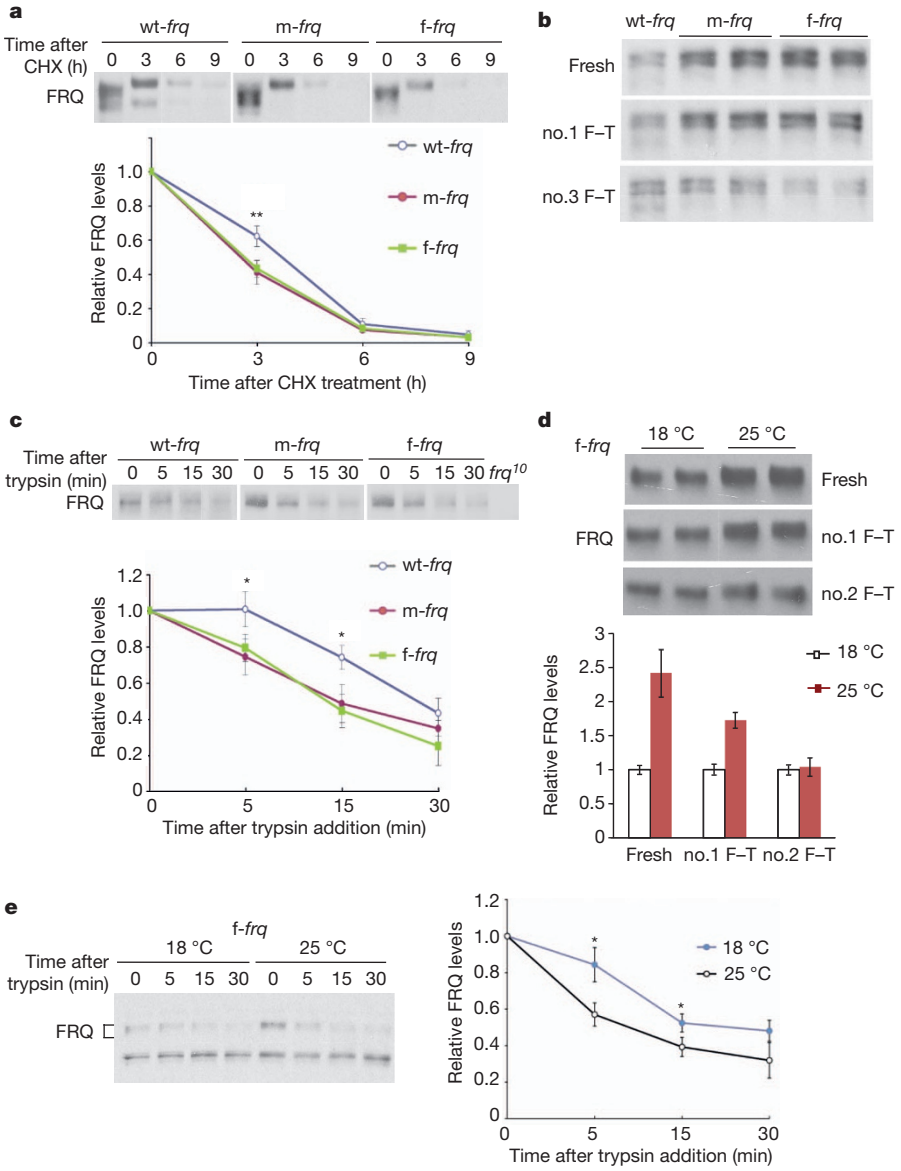

Figure 3 | FRQ protein in the codon-optimized strains is less stable and more sensitive to trypsin digestion. **a**, Top, western blots showing FRQ degradation after CHX treatment (10 μg ml^{-1}). A longer exposure for the wt-*frq* strain was used so that the FRQ signals at time 0 are comparable between the three strains. Bottom, densitometric analyses of results of four independent experiments. **b**, **c**, Western blots showing sensitivity of FRQ from codon-optimized strains to freeze–thaw (F–T) cycles (**b**) and trypsin (1 μg ml) digestion (**c**, top). A longer exposure for the wt-*frq* strain was used in **c**. Densitometric analyses of FRQ levels of three independent experiments are shown (**c**, bottom). **d**, **e**, Western blots showing that FRQ from the f-*frq* strain grown at 18 °C is more resistant to freeze–thaw cycles (**d**; $n = 2$) and to trypsin digestion (**e**; $n = 4$) than that grown at 25 °C. *$P < 0.05$, **$P < 0.01$. For **d** and **e**, the densitometric analyses of the results are also shown. Error bars in **a**, **c**, **e** denote ± s.d.

18 °C, as low temperature is known to reduce FRQ expression[21] (Fig. 4d). The low-temperature treatment was not successful in restoring the circadian conidiation rhythm of the f-*frq* strain (data not shown), which was not surprising because 18 °C is near the lower limit of temperature range permissive for rhythmicity[22]. FRQ in the f-*frq* strain at 18 °C, however, is much less sensitive to freeze–thaw cycles and to trypsin digestion than at 25 °C (Fig. 3d, e). These results suggest that *frq* codon optimization changes FRQ structure as a consequence of increasing translation rate.

To determine whether the codon-usage effect on FRQ is limited to the N terminus of FRQ, we created a mid-*frq* strain, in which the middle region (amino acids 185–530) of the *frq* ORF is optimized. This region contains two casein kinase 1 (CK1)-interaction domains and most of the phosphorylation sites that are important for FRQ stability and period determination[23,24]. Thus, changes of FRQ structural conformation in this region should affect FRQ phosphorylation and stability. As with m-*frq* and f-*frq* strains, the mid-*frq* strain exhibited arrhythmic conidiation (Fig. 4a). In the mid-*frq* strain, FRQ levels were high, and FRQ levels and phosphorylation profile were not rhythmic (Fig. 4b, c). No significant difference in *frq* mRNA was observed (Supplementary Fig. 7). Notably, in the mid-*frq* strain, FRQ accumulated in hypophosphorylated forms, was more stable after CHX treatment and was more resistant to trypsin digestion (Fig. 4b–e). In addition, the CHX-triggered rapid hyperphosphorylation of FRQ in the wt-*frq* strain was abolished in the mid-*frq* strain[22]. These results strongly indicate that the non-optimal codon usage of *frq* is important for FRQ structural required for proper phosphorylation and stability. The opposite molecular phenotypes of mid-*frq* and the N-terminal-optimized strains indicate that changes in FRQ structural conformation in these strains are due to location-specific codon optimization.

In a companion study, codon optimization of *kaiBC* clock genes in cyanobacteria results in high Kai protein levels and impaired cell growth at cool temperatures[25], suggesting that non-optimal codon usage is a shared adaptive mechanism in both prokaryotes and eukaryotes.

Our study suggests that codon usage regulates not only protein-expression level but also its structure and function. Protein folding, which occurs cotranslationally, requires protein chaperones and sufficient amounts of time[17]. Codon optimization results in increased translation rates and thus reduces the time available for folding. Bioinformatics analyses and heterologous protein-expression studies previously implicated codon usage as a factor that regulates protein folding[26–28]. In addition, a single rare codon in the human *MDR1* (also known as *ABCB1*) gene results in altered drug and inhibitor interaction[29].

In sharp contrast with the cyanobacterial Kai proteins[30], most of the FRQ protein is predicted to be disordered (Supplementary Fig. 8). Interestingly, the known domains of FRQ all have relatively low disorder tendencies and fall in regions where codon-usage scores are relatively high, suggesting that a fast translation rate in these well-structured regions does not interfere with protein folding. On the other hand, although the disordered regions may not form stable structures by themselves, they are critical for proper FRQ phosphorylation and

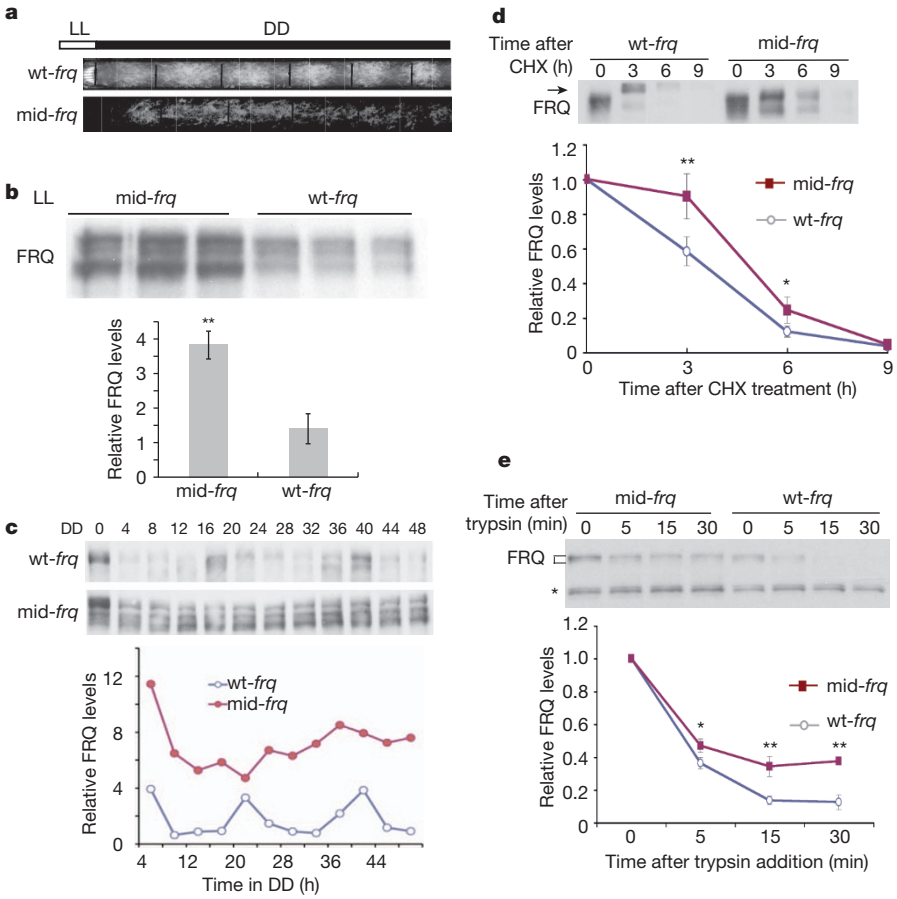

Figure 4 | Codon optimization of the middle region of FRQ impairs FRQ phosphorylation and stabilizes FRQ. **a**, Race tube analysis showing the conidiation phenotypes of indicated strains in constant darkness. **b**, Top, western blot showing FRQ expression profile in constant light. Bottom, densitometric analyses of three independent samples. **c**, Top, western blots showing FRQ expression profile in constant darkness. Bottom, densitometric analysis of the result. **d**, Top, western blot showing the degradation of FRQ after CHX treatment. The arrow indicates the hyperphosphorylated forms of FRQ after the addition of CHX in the wt-*frq* strain. Bottom, densitometric analyses from four independent experiments. **e**, Top, western blot showing reduced sensitivity of FRQ from mid-*frq* to trypsin digestion (2 μg ml^{-1}). Bottom, densitometric analyses of three independent experiments. Error bars denote s.d. $*P < 0.05$, $**P < 0.01$.

stability[23,24]. They may serve as platforms for inter- or intramolecular protein–protein interactions, which may require more time for protein folding than well-structured domains. Therefore, *frq* non-optimal codon usage should be a mechanism that allows the proper folding of FRQ by reducing translation rate in these predicted disordered regions.

METHODS SUMMARY

Codons were optimized on the basis of *Neurospora* codon-usage frequency. Codon-usage score plot was obtained using software Codon Usage 3.5 (developed by Conrad Halling). CBI, frequency of optimal codons (Fop), ENC (effective number of codons) and GC (guanine-cytosine) content values were calculated by codonw (http://mobyle.pasteur.fr/cgi-bin/portal.py#forms::codonw). Optimized *frq* constructs were transformed into a *bd*, frq^{10}, *his-3* strain.

Full Methods and any associated references are available in the online version of the paper.

Received 31 May; accepted 11 December 2012.
Published online 17 February 2013.

1. Ikemura, T. Codon usage and tRNA content in unicellular and multicellular organisms. *Mol. Biol. Evol.* **2,** 13–34 (1985).
2. Plotkin, J. B. & Kudla, G. Synonymous but not the same: the causes and consequences of codon bias. *Nature Rev. Genet.* **12,** 32–42 (2011).
3. Drummond, D. A. & Wilke, C. O. Mistranslation-induced protein misfolding as a dominant constraint on coding-sequence evolution. *Cell* **134,** 341–352 (2008).
4. Tuller, T. *et al.* An evolutionarily conserved mechanism for controlling the efficiency of protein translation. *Cell* **141,** 344–354 (2010).
5. Gu, W., Zhou, T. & Wilke, C. O. A universal trend of reduced mRNA stability near the translation-initiation site in prokaryotes and eukaryotes. *PLoS Comput. Biol.* **6,** e1000664 (2010).
6. Cannarozzi, G. *et al.* A role for codon order in translation dynamics. *Cell* **141,** 355–367 (2010).
7. Heintzen, C. & Liu, Y. The *Neurospora crassa* circadian clock. *Adv. Genet.* **58,** 25–66 (2007).
8. Baker, C. L., Loros, J. J. & Dunlap, J. C. The circadian clock of *Neurospora crassa*. *FEMS Microbiol. Rev.* **36,** 95–110 (2012).
9. Cheng, P., He, Q., He, Q., Wang, L. & Liu, Y. Regulation of the *Neurospora* circadian clock by an RNA helicase. *Genes Dev.* **19,** 234–241 (2005).
10. Cheng, P., Yang, Y. & Liu, Y. Interlocked feedback loops contribute to the robustness of the *Neurospora* circadian clock. *Proc. Natl Acad. Sci. USA* **98,** 7408–7413 (2001).
11. He, Q. *et al.* CKI and CKII mediate the FREQUENCY-dependent phosphorylation of the WHITE COLLAR complex to close the *Neurospora* circadian negative feedback loop. *Genes Dev.* **20,** 2552–2565 (2006).
12. Schafmeier, T. *et al.* Transcriptional feedback of *Neurospora* circadian clock gene by phosphorylation-dependent inactivation of its transcription factor. *Cell* **122,** 235–246 (2005).
13. Huang, G., Wang, L. & Liu, Y. Molecular mechanism of suppression of circadian rhythms by a critical stimulus. *EMBO J.* **25,** 5349–5357 (2006).
14. Lee, K., Loros, J. J. & Dunlap, J. C. Interconnected feedback loops in the *Neurospora* circadian system. *Science* **289,** 107–110 (2000).
15. Morgan, L. W., Greene, A. V. & Bell-Pedersen, D. Circadian and light-induced expression of luciferase in *Neurospora crassa*. *Fungal Genet. Biol.* **38,** 327–332 (2003).
16. Gooch, V. D. *et al.* Fully codon-optimized luciferase uncovers novel temperature characteristics of the *Neurospora* clock. *Eukaryot. Cell* **7,** 28–37 (2008).
17. Spencer, P. S., Siller, E., Anderson, J. F. & Barral, J. M. Silent substitutions predictably alter translation elongation rates and protein folding efficiencies. *J. Mol. Biol.* **422,** 328–335 (2012).
18. Bennetzen, J. L. & Hall, B. D. Codon selection in yeast. *J. Biol. Chem.* **257,** 3026–3031 (1982).
19. Colot, H. V., Loros, J. J. & Dunlap, J. C. Temperature-modulated alternative splicing and promoter use in the circadian clock gene *frequency*. *Mol. Biol. Cell* **16,** 5563–5571 (2005).
20. Diernfellner, A. *et al.* Long and short isoforms of *Neurospora* clock protein FRQ support temperature-compensated circadian rhythms. *FEBS Lett.* **581,** 5759–5764 (2007).
21. Liu, Y., Merrow, M. M., Loros, J. J. & Dunlap, J. C. How temperature changes reset a circadian oscillator. *Science* **281,** 825–829 (1998).
22. Liu, Y., Garceau, N., Loros, J. J. & Dunlap, J. C. Thermally regulated translational control mediates an aspect of temperature compensation in the *Neurospora* circadian clock. *Cell* **89,** 477–486 (1997).
23. Tang, C. T. *et al.* Setting the pace of the *Neurospora* circadian clock by multiple independent FRQ phosphorylation events. *Proc. Natl Acad. Sci. USA* **106,** 10722–10727 (2009).
24. Baker, C. L., Kettenbach, A. N., Loros, J. J., Gerber, S. A. & Dunlap, J. C. Quantitative proteomics reveals a dynamic interactome and phase-specific phosphorylation in the *Neurospora* circadian clock. *Mol. Cell* **34,** 354–363 (2009).
25. Xu, Y., Ma, P., Shah, P., Rokas, A., Liu, Y. & Johnson, C. H. Non-optimal codon usage is a mechanism to achieve circadian clock conditionality. *Nature* http://dx.doi.org/10.1038/nature11942 (this issue).
26. Zhou, T., Weems, M. & Wilke, C. O. Translationally optimal codons associate with structurally sensitive sites in proteins. *Mol. Biol. Evol.* **26,** 1571–1580 (2009).
27. Siller, E., DeZwaan, D. C., Anderson, J. F., Freeman, B. C. & Barral, J. M. Slowing bacterial translation speed enhances eukaryotic protein folding efficiency. *J. Mol. Biol.* **396,** 1310–1318 (2010).
28. Komar, A. A., Lesnik, T. & Reiss, C. Synonymous codon substitutions affect ribosome traffic and protein folding during *in vitro* translation. *FEBS Lett.* **462,** 387–391 (1999).
29. Kimchi-Sarfaty, C. *et al.* A "silent" polymorphism in the *MDR*1 gene changes substrate specificity. *Science* **315,** 525–528 (2007).
30. Johnson, C. H., Stewart, P. L. & Egli, M. The cyanobacterial circadian system: from biophysics to bioevolution. *Annu. Rev. Biophys.* **40,** 143–167 (2011).

Supplementary Information is available in the online version of the paper.

Acknowledgements We thank H. Yuan and Q. Ye for technical assistance, J. Dunlap for providing the p*frq-luc-I* construct and M. Rosbash for suggesting the temperature experiments. We apologize to those colleagues whose studies we could not cite owing to space limitations. This work was supported by grants from the National Institutes of Health to Y.L. (GM068496 & GM062591) and M.S.S. (GM47498), and from the Welch Foundation (I-1560) to Y.L.

Author Contributions Y.L., M.Z. and J.G. designed the research. M.Z., J.G., J.C., M.C., S.C. and J.M.B. performed experiments. M.Z., J.G., J.M.B., M.S.S. and Y.L. analysed the results. Y.L. and M.Z. wrote the paper; J.G., J.M.B. and M.S.S. edited and commented on the manuscript.

Author Information Reprints and permissions information is available at www.nature.com/reprints. The authors declare no competing financial interests. Readers are welcome to comment on the online version of the paper. Correspondence and requests for materials should be addressed to Y.L. (Yi.Liu@UTsouthwestern.edu).

METHODS

Strains and growth conditions. *Neurospora* strains used in this study were 87-3 (*bd a*; clock wild-type), 303-3 (*bd*, frq^{10}, *his-3*)[31] and different *frq* N-terminal-codon-optimized strains created in this study. Strain 303-3 was used as the host strain for various *his-3*-targeting constructs. The frq^{10}, *bd*, wt-*frq* (frq^{10} containing a wild-type *frq* gene at the *his-3* locus) strain was used as the control in this study.

Growth conditions have been described previously[32]. Liquid cultures were grown in minimal medium (1 × Vogel's, 2% glucose). When quinic acid was used, liquid cultures were grown in (10^{-6}–10^{-2} M) quinic acid, pH 5.8, 1 × Vogel's, 0.1% glucose and 0.17% arginine. Race tube media contained 1 × Vogel's, 0.1% glucose, 0.17% arginine, 50 ng ml^{-1} biotin and 1.5% agar. For rhythmic experiments, the *Neurospora* cultures were transferred from LL to DD at time 0 and were collected in DD at the indicated time (hours). Calculations of period length were performed as described[22].

***frq* codon optimization, codon-usage score plot and indices calculation.** *frq* codon optimization was performed for the N-terminal part (1–498 nucleotides) or the middle region (553–1,590 nucleotides) of the ORF. The nucleotide sequences of the optimized *frq* are shown in Supplementary Figs 9 and 10. Codons were optimized on the basis of *N. crassa* codon-usage frequency and the predicted most efficient codon on the basis of tRNA copy numbers. In total, 65 codons were optimized in the m-*frq* construct, whereas 94 codons were optimized in the f-*frq* construct. Sequences surrounding an alternative *frq* 3′ splice site in this region were not mutated.

Codon-usage score plot was obtained using Codon Usage 3.5 (developed by Conrad Halling) using a window size of 35 and logarithmic range of 3. The *N. crassa* codon-usage frequency table was obtained from http://www.kazusa.or.jp/codon/. To calculate the CBI, frequency of optimal codons (Fop), ENC (effective number of codons) and GC (guanine-cytosine) content, codonw in the Mobyle Portal website (http://mobyle.pasteur.fr/cgi-bin/portal.py#forms::codonw) was used[18,33]. CBI will equal 1.0 if a gene has extreme codon bias and will equal 0 if codon usage is completely random. If the number of optimal codons is less than expected by random change, the CBI value will be a negative value. *Neurospora* genome sequences were downloaded from the Broad Institute *N. crassa* database (http://www.broadinstitute.org/annotation/genome/neurospora/MultiHome.html). The top 100 most abundant proteins were identified by mass spectrometry analyses and ranked by their emPAI (exponentially modified protein abundance index) values[34] (Supplementary Table 1).

Plasmid constructs and *Neurospora* transformation. pKAJ120 (containing the entire wild-type *frq* gene including its promoter and a *his-3*-targeting sequence) and pBA50 (containing the wild-type *frq* gene under the control of the *qa-2* promoter and a *his-3*-targeting sequence) were used as the parental plasmids to create the optimized *frq* constructs[32]. Optimized *frq* sequences (synthesized by Genscript) were subcloned into parental plasmids to replace the wild-type *frq* gene to generate the m-*frq*, f-*frq* and mid-*frq* constructs. In the m1-*frq* construct, only the codons upstream of the predicted intron branch point were optimized as m-*frq*. For the m2-*frq* construct, only the codons downstream of the intron 3′ end were optimized as m-*frq*. The resulting constructs were transformed into strain 303-3 by electroporation and targeted to the *his-3* locus[35]. Homokaryon strains were obtained by microconidia purification.

Protein and RNA analyses. Protein extraction, western blot analysis and immunoprecipitation assays were performed as previously described[36–38]. Equal amounts of total protein (50 μg) were loaded into each lane of SDS–PAGE gels (7.5% SDS–PAGE gels containing a ratio of 37.5:1 acrylamide/bisacrylamide). Densitometry of the signal was performed by using Image J.

RNA extraction and quantitative reverse transcriptase PCR (qRT–PCR) were performed as previously described[39,40]. For qRT–PCR, the primer sequences used for *frq* were 5′-GGAGGAGTCGATGTCACAAGG-3′ (forward) and 5′-CACTTCGAGTTACCCATGTTGC-3′ (reverse). The *Neurospora* gene coding for β-tubulin was used as an internal control. The primer sequences specific for β-tubulin were 5′-GCGTATCGGCGAGCAGTT-3′(forward) and 5′-CCTCACCAGTGTACCAATGCA-3′ (reverse).

frq mRNA secondary structure and folding energy was predicted by the mfold program (http://mfold.rna.albany.edu/?q=mfold/RNA-Folding-Form).

Mass spectrometric analyses and database search. The *Neurospora* proteins were separated on a 4–20% SDS–PAGE gradient gel. The whole-protein gel lane was sliced equally into 14 gel blocks from top to bottom. Each gel block was destained and then digested in-gel with sequencing grade trypsin (10 ng μl^{-1} trypsin in 50 mM ammonium bicarbonate, pH 8.0) at 37 °C overnight. The resulting tryptic peptides from each gel block were extracted with 5% formic acid/50% acetonitrile and 0.1% formic acid/75% acetonitrile sequentially and then concentrated to ~20 μl in a CentriVap system (Labconco). The extracted peptides from each sample were separated by a home-made analytical capillary column (50 μm × 10 cm) packed with 5-μm spherical C18 reversed-phase material (YMC). An Agilent 1100 binary pump was used to generate high-performance liquid chromatography gradient as follows: 0–5% B in 5 min, 5–40% B in 55 min, 40–100% B in 15 min (A = 0.2 M acetic acid in water; B = 0.2 M acetic acid/70% acetonitrile). The eluted peptides were sprayed directly into a LTQ mass spectrometer (Thermo Fisher Scientific) equipped with a nano-ESI ion source. The mass spectrometer was operated in data-dependent mode (MS scan mass range was 350–2,000 Da, the top-five most abundant precursor ions from each MS scan were selected for MS–MS scans, and dynamic exclusion time was 30 s). The mass spectrometric data from all 14 samples were combined and searched against *Neurospora* protein database on an in-house Mascot server (Matrix Science). The main search parameters were as below: protein N-terminal acetylation and methionine oxidation were included as variable modifications; two missed cleavage sites were allowed; precursor ion mass tolerance was set as 3 Da; fragment ion mass tolerance was 0.8 Da. Only peptides with *E* value above 0.01 were retained. The emPAI[34] was calculated for each protein by the Mascot software.

Luciferase reporter assay. The luciferase reporter construct (*frq-luc-bar*) was generated by insertion of the 4.7-kb BamHI-NotI fragment of p*frq-luc-I* (a generous gift from J. Dunlap)[16] into the corresponding sites of pBARKS1. This construct, which contains the luciferase gene under the control of the *frq* promoter and the *bar* gene, was transformed into 87-3 (*bd a*), wt-*frq* (frq^{10}, *bd*, wt-*frq*), m-*frq* (frq^{10}, *bd*, m-*frq*) and f-*frq* (frq^{10}, *bd*, f-*frq*) strains. Transformants were selected using the basta/ignite (200 μg ml^{-1}) resistance conferred by the *bar* gene.

LumiCycle (Actimetrics) was used for the luciferase assay using a protocol similar to previously described[16]. The AFV (autoclaved FGS-Vogel's) medium contained 1 × FGS (0.05% fructose, 0.05% glucose, 2% sorbose), 1 × Vogel's medium, 50 μg l^{-1} biotin and 1.8% agar. Firefly luciferin (L-8200 D-luciferin firefly (synthetic) potassium salt; BioSynth) was added to the medium after autoclaving (final concentration 50 μM). One drop of conidia suspensions in water were placed on AFV medium and grown in LL overnight. The cultures were then transferred to darkness, and luminescence was recorded in real time DD using a LumiCycle after 1 day in DD. The data were then normalized with LumiCycle analysis software by subtracting the baseline luciferase signal, which increases as cell grows. Therefore, the normalized luciferase signals reflect the amplitude of the rhythm and do not reflect the absolute luciferase signal. Under our experimental conditions, luciferasae signals were highly variable during the first day in the LumiCycle and became stabilized afterwards, which is probably because of an artefact caused by the light–dark transfer of the cultures. Thus, the results presented were recorded after 1 day in DD.

Protein-stability assay. The liquid cultures of *Neurospora* strains were grown in LL for 1 day before the addition of CHX (final concentration 10 μg ml^{-1}). Cells were collected at the indicated time points.

For the trypsin-sensitivity assay, protein extracts were diluted to a protein concentration of 2.5 μg μl^{-1}. 100-μl extracts were treated with trypsin (final concentration 1 μg ml^{-1}) at 25 °C. A 20-μl sample was taken from the reaction at each time point (0, 5, 15 and 30 min) after addition of trypsin. Protein samples were mixed with protein loading buffer and resolved by SDS–PAGE. To compare trypsin sensitivity of FRQ from different strains, experiments were performed side by side and the protein samples were transferred to the same membrane for western blot analysis.

31. Cha, J., Yuan, H. & Liu, Y. Regulation of the activity and cellular localization of the circadian clock protein FRQ. *J. Biol. Chem.* **286,** 11469–11478 (2011).
32. Aronson, B. D., Johnson, K. A., Loros, J. J. & Dunlap, J. C. Negative feedback defining a circadian clock: autoregulation in the clock gene *frequency*. *Science* **263,** 1578–1584 (1994).
33. Wright, F. The 'effective number of codons' used in a gene. *Gene* **87,** 23–29 (1990).
34. Ishihama, Y. *et al.* Exponentially modified protein abundance index (emPAI) for estimation of absolute protein amount in proteomics by the number of sequenced peptides per protein. *Mol. Cell. Proteomics* **4,** 1265–1272 (2005).
35. Bell-Pedersen, D., Dunlap, J. C. & Loros, J. J. Distinct *cis*-acting elements mediate clock, light, and developmental regulation of the *Neurospora crassa eas* (*ccg-2*) gene. *Mol. Cell. Biol.* **16,** 513–521 (1996).
36. Cheng, P., Yang, Y., Heintzen, C. & Liu, Y. Coiled-coil domain mediated FRQ–FRQ interaction is essential for its circadian clock function in *Neurospora*. *EMBO J.* **20,** 101–108 (2001).
37. Garceau, N. Y., Liu, Y., Loros, J. J. & Dunlap, J. C. Alternative initiation of translation and time-specific phosphorylation yield multiple forms of the essential clock protein FREQUENCY. *Cell* **89,** 469–476 (1997).
38. Guo, J., Cheng, P., Yuan, H. & Liu, Y. The exosome regulates circadian gene expression in a posttranscriptional negative feedback loop. *Cell* **138,** 1236–1246 (2009).
39. Crosthwaite, S. K., Loros, J. J. & Dunlap, J. C. Light-Induced resetting of a circadian clock is mediated by a rapid increase in *frequency* transcript. *Cell* **81,** 1003–1012 (1995).
40. Choudhary, S. *et al.* A double-stranded-RNA response program important for RNA interference efficiency. *Mol. Cell. Biol.* **27,** 3995–4005 (2007).